Optical Engineering 44(11), 1 (November 2005)

Two-dimensional continuous higher-order energy operators

Abdel-Ouahab Boudraa
Ecole Navale
IRENav
29240 Brest-Armées, France
E-mail: boudra@ecole-navale.fr

Fabien Salzenstein
Université de Strasbourg
Laboratoire Phase-CNRS
23 rue du Loess
Strasbourg, France

Jean-Christophe Cexus
Ecole Navale
IRENav
29240 Brest-Armées, France

Abstract. An extension of the 2-D discrete Teager-Kaiser energy operator and the 1-D higher-order energy operators to the 2-D continuous case is proposed. These 2-D continuous operators are flexible enough to apply a large class of image gradient filters, and consequently different discrete energy operators are derived. Particularly, the proposed model takes into account the diagonal directions, through the partial derivatives. The obtained operators are computationally very simple, like the classical 2D Teager-Kaiser operator, and are well suited for image-processing applications such as image demodulation or image contrast enhancement. Results of demodulation of synthetic and real images, to estimate envelope information, are presented to show the feasibility of the proposed operators. © *2005 Society of Photo-Optical Instrumentation Engineers.* [DOI: 10.1117/1.2128125]

Subject terms: AM-FM model; Teager-Kaiser energy operator; 2-D modulation; higher-order energy operators; image demodulation.

Paper 040664RR received Sep. 13, 2004; revised manuscript received Mar. 16, 2005 and Apr. 26, 2005; accepted for publication Apr. 28, 2005. A part of this work has been presented at the Seventh International Symposium on Signal Processing and its Applications (ISSPA), Paris, France, 2003.

1 Introduction

Amplitude modulation (AM) and frequency modulation (FM) signals are widely used for modeling and transmission of information over communication channels. Such signals have also been used to model time-varying amplitude and frequency patterns in speech resonances, where each formant is represented by an AM-FM signal.[1] To demodulate a monocomponent AM-FM signal into its amplitude envelope and instantaneous frequency, the energy separation algorithm (ESA) based on the Teager-Kaiser energy operator (TKEO)[2] has been proposed.[1] The TKEO owes its energy-tracking capability to the fact that when it is applied to the output signal from a simple harmonic oscillator, it tracks the energy of the source, generating the signal.[2] Maragos et al.[1] referred to the TKEO as the nonlinear energy-tracking signal operator. The TKEO has been extended to two-dimensional (2-D) signals by Yu et al.[3] and has found applications in image processing, such as image demodulation,[4,5] image segmentation,[6] noise reduction,[7] and image contrast enhancement.[8–10]

Higher-order generalization of the TKEO to continuous and discrete times have been proposed by Maragos and Potamianos.[11] We have recently extended these operators to the 2-D discrete case.[5] To our knowledge, there has been very little work on continuous extension of the 2-D TKEO and the high-order energy operators. In this paper, we introduce such continuous operators, which are flexible enough to include a large class of image gradient filters. The continuous information increases the choice of discrete energy operators. Particularly, the cross-diagonal directions, using partial first and second derivatives, are taken into account. Because these continuous operators are also computationally very simple, they are well suited for image-processing applications such as image demodulation, contrast enhancement, and noise filtering. For example, 2-D demodulation provides a rich description of local texture structures of an image.

2 The Teager-Kaiser Energy Operator

2.1 *1-D Continuous and Discrete Energy Operators*

For a one-dimensional (1-D) continuous signal $s(t)$, the TKEO Ψ is defined by[2]

$$\Psi[s(t)] = \left[\frac{\partial s(t)}{\partial t}\right]^2 - s(t)\frac{\partial^2 s(t)}{\partial t^2}. \tag{1}$$

This operator, which is homogeneous to an energy, is particularly useful and efficient for demodulating a given wave: it is easy to show that the output for a pure sinusoidal signal $s(t)=A\cos\omega t$ is $\Psi[s(t)]=A^2\omega^2$. Thus, the TKEO output for a monochromatic source gives an energy that is proportional to the square of the amplitude and frequency. The discrete version of this operator is given, according to the discrete approximations of the first and second derivatives, by[2]

$$\Psi[s(n)] = s^2(n) - s(n+1)s(n-1). \tag{2}$$

A large class of discrete versions of the TKEO exist,[12] but the symmetrical version, given by Eq. (2), is the most used in practice. Again, the discrete Teager-Kaiser energy of a pure sinusoidal signal $s(n)=A\cos(\omega_0 n+\alpha)$ is $A^2\omega_0^2$, a quantity that is proportional to the signal energy. Thus, using the TKEO, we can estimate the amplitude and frequency values of a modulated signal. Generally, for a local discrete signal $s(n)=a(n)\cos\varphi(n)$, Eq. (2) yields

$a^2(n)\dot{\varphi}^2(n)$. This gives the instantaneous frequency and envelope. Algorithms such as the ESA extract the frequency and envelope information at a given time, by computing the Teager-Kaiser function Ψ of a monochromatic signal and its discrete derivatives, respectively.[1] Note that the TKEO is limited to monocomponent signals.

2.2 *2-D Discrete Teager-Kaiser Energy Operator*

The TKEO, originally defined for 1-D signals, has been extended to 2-D by Yu et al.[3] This extension is limited to the discrete case. By applying Eq. (2) independently to the horizontal, diagonal, and vertical directions of an image $(s(k,l))_{1\leq k\leq N,1\leq l\leq N}$ and summing the results, one obtains two 2-D discrete versions of the TKEO[3]:

$$\Psi_2[s(k,l)] = 2s^2(k,l) - s(k-1,l)s(k+1,l) - s(k,l-1)s(k,l+1), \tag{3}$$

$$\Psi_2[s(k,l)] = 2s^2(k,l) - s(k+1,l-1)s(k-1,l+1) - s(k+1,l+1)s(k-1,l-1). \tag{4}$$

Equations (3) and (4) are called type 1A-Q and type 1B-Q filters, respectively.[3] The subscript of Ψ indicates the order of the operator. These two filters have been used for image contrast enhancement and give better results than conventional unsharp masking based on linear 2-D highpass filters.[3,10] Furthermore, it has been shown that these two filters are simple second-order Volterra filters.[8] For an image modeled as a 2-D spatial AM-FM signal, $s(k,l) = a(k,l)\cos\varphi(k,l)$, Eq. (3) approximates the multidimensional Teager-Kaiser energy $a^2(k,l)\nabla^2\varphi(k,l)$.[4,6] A modified version of the 2-D TKEO has been introduced, by adding Eqs. (3) and (4), for detecting surface roughness in white light scanning interferometry.[5]

3 Higher-Order Differential Energy Operators

In Ref. 11, Maragos and Potamianos proposed a generalization of the 1-D TKEO, called the k'th-order differential energy operator (DEO), yielding the cross energy between a signal $s(t)$ and its $(k-1)$'th derivative:

$$\Psi_k[s(t)] = \frac{\partial s(t)}{\partial t}\frac{\partial^{k-1}s(t)}{\partial t^{k-1}} - s(t)\frac{\partial^k s(t)}{\partial t^k}. \tag{5}$$

Thus, the TKEO corresponds to the second-order DEO. More generally, there is a recursive relation between the k'th-order operator and the lower-order ones:

$$\Psi_k[s(t)] = \frac{\partial\Psi_{k-1}[s(t)]}{\partial t} - \Psi_{k-2}\left[\frac{\partial s(t)}{\partial t}\right]. \tag{6}$$

Applying Ψ_k to a pure sinusoidal signal $s(t)=A\cos(\omega t+\alpha)$ gives the following outputs[11]:

$$\Psi_k[s(t)] = \begin{cases} 0 & \text{if } k = \pm 1, \pm 3 \ldots, \\ (-1)^{1+k/2}A^2\omega^k & \text{if } k = 0, \pm 2, \pm 4, \ldots. \end{cases}$$

In particular combining the fourth- and second-order DEOs leads to the instantaneous phase and frequency of a simple AM-FM signal. Finally, the discrete associated nonlinear functions depend on the choice of the discrete partial derivatives.

The proposed generalization of the discrete Teager-Kaiser energy function in Ref. 11 leads to an asymmetric k'th-order operator Ψ_k:

$$\Psi_k[s(n)] = s(n)s(n+k-2) - s(n-1)s(n+k-1). \tag{7}$$

In Ref. 5, we have extended the DEO to the 2-D case, called discrete 2-D DEO (D2DEO), in order to improve the extraction of the fringe envelope to detect the surface height of a material. For instance, the third- and the fourth-order D2DEO (3- and 4D2DEO) are described as follows:

$$\Psi_3[s(k,l)] = s(k,l)s(k+1,l) - s(k-1,l)s(k+2,l) + s(k,l)s(k,l+1) - s(k,l-1)s(k,l+2), \tag{8}$$

$$\Psi_4[s(k,l)] = s(k,l)s(k+2,l) - s(k-1,l)s(k+3,l) + s(k,l)s(k,l+2) - s(k,l-1)s(k,l+3). \tag{9}$$

Note that both Eqs. (8) and (9) are limited to two directions. It would be possible to include diagonal directions.

4 2-D Continuous Energy Operators

In this section, new continuous energy operators for 2-D signal processing are introduced. The proposed Teager-Kaiser energy and high-order energy operators are flexible enough to include a large class of image gradient filters. More specifically, the introduction of the gradient filters, instead of using the usual discrete approximations, broadens the choice of the discrete energy operators.

4.1 *2-D Continuous Second-Order Energy Operator*

Let $s(x,y)$ be a 2-D signal. Suppose that $s(x,y)$ possesses continuous partial derivatives along the vertical (x-axis) and horizontal (y-axis) directions. The continuous 2-D DEO (C2DEO), or continuous 2D TKEO (C2TKEO), denoted Φ_2^c, is defined by

$$\Phi_2^c[s(x,y)] = \|\nabla s(x,y)\|^2 - \langle s(x,y)\nabla_2 s(x,y)\rangle, \tag{10}$$

where $\nabla_2 s(x,y)$ represents the Laplacian of the signal, $\|\cdot\|$ is the usual quadratic norm on $\mathbb{R}^2$, and $\langle\cdot\rangle$ is the scalar product. The superscript on Φ indicates the continuous operator version. Equation (10) can be written as

$$\Phi_2^c[s(x,y)] = \left[\left(\frac{\partial s}{\partial x}\right)^2 - s\frac{\partial^2 s}{\partial x^2}\right] + \left[\left(\frac{\partial s}{\partial y}\right)^2 - s\frac{\partial^2 s}{\partial y^2}\right] + 2\left[\left(\frac{\partial s}{\partial x}\frac{\partial s}{\partial y}\right) - s\frac{\partial^2 s}{\partial x\,\partial y}\right]. \tag{11}$$

Note that the first two terms represent the 1-D TKEO along the vertical and the horizontal axis respectively. These terms correspond to the 2-D discrete operator introduced by Maragos and Bovik,[4] while the third term is the cross-derivative term representing the interaction energy between the two coordinates. Finally, the C2DEO (or C2TKEO) gives more possibilities and offers greater flexibility in the choice of its corresponding discrete versions.

4.2 *Response to an AM Signal*

The Teager-Kaiser energy of an AM 1-D signal $s(t)=a(t)\cos \omega t$ is given by

$$\Psi[a(t)\cos \omega t] = a^2(t)\omega^2 + \cos^2 \omega t\, \Psi[a(t)].$$

This relation is composed of a term similar to the energy of a sinusoidal signal and an oscillation governed by the Teager-Kaiser energy of the amplitude. Consider a 2-D AM signal $s(x,y)=a(x,y)\cos(\omega_x x+\omega_y y)$. We have immediately

$$\Phi_2^c[s(x,y)] = a^2(x,y)(\omega_x+\omega_y)^2 + \cos^2(\omega_x x+\omega_y y)\Phi_2^c[a(x,y)], \quad (12)$$

where ω_x and ω_y represent respectively the horizontal and vertical spatial frequencies. Hence, for a pure sinusoidal wave, $a(x,y)$ is constant, we have $\Phi_2^c[a(x,y)]=0$, and thus Eq. (12) is reduced to

$$\Phi_2^c[s(x,y)] = a^2(x,y)(\omega_x+\omega_y)^2. \quad (13)$$

Thus, the demodulation of 2-D continuous signals is possible.

4.3 *2-D Continuous Higher-Order Energy Operators*

As in the 1-D case, let us consider the following nonlinear third-order operator Φ_3^c:

$$\Phi_3^c[s(x,y)] = \nabla s(x,y)\nabla_2 s(x,y) - s(x,y)\nabla_3 s(x,y),$$

where ∇_2 (the Laplacian) and ∇_3 represent respectively the second- and the third-order gradient operators. The output of the 3C2DEO applied to $s(x,y)$ is given by

$$\begin{aligned}\Phi_3^c[s(x,y)] = &\left(\frac{\partial s}{\partial x}\frac{\partial^2 s}{\partial x^2} - s\frac{\partial^3 s}{\partial x^3}\right) + \left(\frac{\partial s}{\partial y}\frac{\partial^2 s}{\partial y^2} - s\frac{\partial^3 s}{\partial y^3}\right)\\ &+ \left(\frac{\partial s}{\partial x}\frac{\partial^2 s}{\partial y^2} + 2\frac{\partial s}{\partial y}\frac{\partial^2 s}{\partial x\,\partial y} - 3s\frac{\partial^3 s}{\partial x\,\partial y^2}\right)\\ &+ \left(\frac{\partial s}{\partial y}\frac{\partial^2 s}{\partial x^2} + 2\frac{\partial s}{\partial x}\frac{\partial^2 s}{\partial x\,\partial y} - 3s\frac{\partial^3 s}{\partial y\,\partial x^2}\right). \quad (14)\end{aligned}$$

Equation (14) contains the 3C2DEO applied to the rows and columns independently, and additional cross-derivative terms. Again, the relation between the 3- and the 2C2DEOs is written as

$$\Phi_3^c[s(x,y)] = \frac{\partial \Phi_2^c[s]}{\partial x} + \frac{\partial \Phi_2^c[s]}{\partial y}. \quad (15)$$

And generally, for a k'th-order operator ($k>3$), we have the following recurrence:

$$\Phi_k^c[s(x,y)] = \frac{\partial \Phi_{k-1}^c[s]}{\partial x} + \frac{\partial \Phi_{k-1}^c[s]}{\partial y} - \Phi_{k-2}^c\left[\frac{\partial s}{\partial x} + \frac{\partial s}{\partial y}\right]. \quad (16)$$

The 3- and 4C2DEOs applied to a pure sinusoidal wave give following the relations[3]:

$$\Phi_3^c[s(x,y)] = 0,$$

$$\Phi_4^c[s(x,y)] = -a(x,y)^2(\omega_x+\omega_y)^4. \quad (17)$$

Both operators Φ_3^c and Φ_4^c allow us to demodulate an AM-FM signal: if the envelope is a slow signal—and so considered as a constant signal locally—Eqs. (13) and (17) give a good approximation of the amplitude:

$$a^2(x,y) = \frac{\{\Phi_2^c[s(x,y)]\}^2}{-\Phi_4^c[s(x,y)]}. \quad (18)$$

The instantaneous spatial frequencies, ω_x and ω_y, are estimated as follows. Suppose that the envelope $a(x,y)\approx a$ is locally constant. The notation $\partial s/\partial x=\dot{s}_x$ and $\partial s/\partial y=\dot{s}_y$ is used. Applying the C2DEO to the signals $\dot{s}_x-\dot{s}_y$ and $\dot{s}_x+\dot{s}_y$, where $s(x,y)=a\cos(\omega_x x+\omega_y y)$, yields immediately

$$\Phi_2^c[\dot{s}_x-\dot{s}_y] = a^2(\omega_x-\omega_y)^2(\omega_x+\omega_y)^2,$$

$$\Phi_2^c[\dot{s}_x+\dot{s}_y] = a^2(\omega_x+\omega_y)^2(\omega_x+\omega_y)^2.$$

Finally, using Eq. (13), we obtain

$$(\omega_x-\omega_y)^2 = \frac{\Phi_2^c[\dot{s}_x-\dot{s}_y]}{\Phi_2^c[s]}, \quad (19)$$

$$(\omega_x+\omega_y)^2 = \frac{\Phi_2^c[\dot{s}_x+\dot{s}_y]}{\Phi_2^c[s]}. \quad (20)$$

Let us now compute the squared norm, $\|\mathbf{w}\|^2=\omega_x^2+\omega_y^2$, of the frequency vector $\mathbf{w}=(\omega_x,\omega_y)$ and its orientation θ, defined by

$$\omega_x = \|\mathbf{w}\|\cos\theta, \qquad \omega_y = \|\mathbf{w}\|\sin\theta. \quad (21)$$

From (19) and (20) we deduce

$$\|\mathbf{w}\|^2 = \frac{\Phi_2^c[\dot{s}_x-\dot{s}_y]+\Phi_2^c[\dot{s}_x+\dot{s}_y]}{2\Phi_2^c[s]}, \quad (22)$$

$$\theta = \frac{1}{2}\arcsin\frac{\Phi_2^c[\dot{s}_x+\dot{s}_y]-\Phi_2^c[\dot{s}_x-\dot{s}_y]}{\Phi_2^c[\dot{s}_x+\dot{s}_y]+\Phi_2^c[\dot{s}_x-\dot{s}_y]}. \quad (23)$$

Equations (18) and (21)–(23) are the steps in fully demodulating the spatial signal $s(x,y)$. We call these relations the continuous higher-order demodulation algorithm (CHOEDA). As for the ESA, the basic assumption behind the ability of the CHOEDA to demodulate the spatial signals is that the input signal is narrowband.

4.4 *Discretization of 2-D Energy Operators*

4.4.1 *Sampling frequency and modulated images*

Examination of Eq. (11) shows that the C2TKEO combines the usual TKEO along the vertical and horizontal directions and partial derivatives along the diagonal direction. The discrete version of the C2TKEO is formulated as follows:

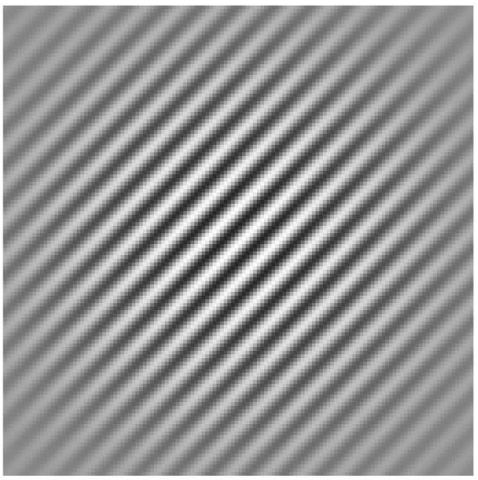

(a)

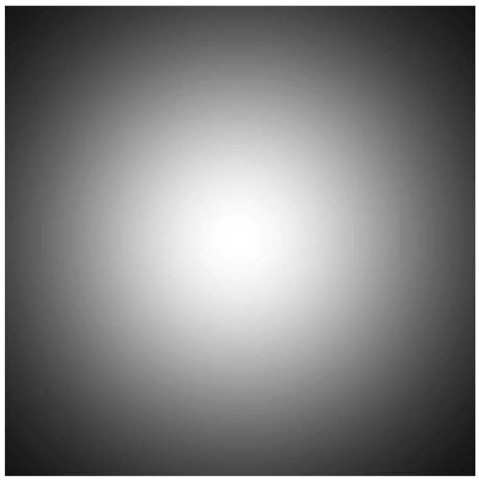

(b)

Fig. 1 Detected envelope of the synthetic image: original Gabor wavelet image (a) and the corresponding envelope image (b).

$$\Phi_2[s(i,j)] = 2s^2(i,j) - s(i-1,j)s(i+1,j) - s(i,j-1)s(i,j+1) + 2[s_x(i,j)s_y(i,j) - s(i,j)s_{xy}(i,j)], \quad (24)$$

where $s_x(i,j)[s_y(i,j)]$ represents the first derivative along $x[y]$, and $s_{xy}(i,j)$ represents the second derivative with respect to x and y. The first line of Eq. (24) corresponds to the 2-D discrete energy operator described by Maragos and Bovik [Ref. 4, Eq. (47), p. 1872] and is identical to the discrete energy operator developed in Ref. 3 for digital image edge detection.

Consider an AM locally modulated signal $s(i,j) = a(i,j)\cos(\Omega_x i + \Omega_y j)$, where $\Omega_x = \omega_x x_e$, $\Omega_y = \omega_y y_e$. The variable $x_e(y_e)$ represents the sampling period along the x axis (the y axis). The assumption that the amplitude $a(i,j)$ is varying more slowly than the carrier signal $\cos(\Omega_x i + \Omega_y j)$ (locally constant) yields immediately

$$s_x(i,j) = \frac{s(i+1,j) - s(i-1,j)}{2} \approx -a(i,j)\sin\Omega_x \sin(\Omega_x i + \Omega_y j),$$

$$s_y(i,j) = \frac{s(i,j+1) - s(i,j-1)}{2} \approx -a(i,j)\sin\Omega_y \sin(\Omega_x i + \Omega_y j),$$

$$s_{xy}(i,j) = \frac{s_y(i+1,j) - s_y(i-1,j)}{2} \approx -a(i,j)\sin\Omega_x \sin\Omega_y \cos(\Omega_x i + \Omega_y j).$$

Finally, a discrete version of the C2TKEO, where the amplitude $a(i,j)$ is locally constant, is given by

$$\begin{aligned}\Phi_2[a(i,j)\cos(\Omega_x i + \Omega_y j)] &= a^2(i,j)\sin^2\Omega_x + a^2(i,j)\sin^2\Omega_y \\ &\quad + 2a^2(i,j)\sin\Omega_x \sin\Omega_y \sin^2(\Omega_x i + \Omega_y j) \\ &\quad + 2a^2(i,j)\sin\Omega_x \sin\Omega_y \cos^2(\Omega_x i + \Omega_y j) \\ &= a^2(i,j)(\sin\Omega_x + \sin\Omega_y)^2. \end{aligned} \quad (25)$$

The same discrete gradient approximations leads to

$$\Phi_3[a(i,j)\cos(\Omega_x i + \Omega_y j)] = 0,$$

$$\Phi_4[a(i,j)\cos(\Omega_x i + \Omega_y j)] = -\Phi_2[s_x(i,j) + s_y(i,j)] = -a^2(i,j)(\sin\Omega_x + \sin\Omega_y)^4. \quad (26)$$

Thus Eqs. (25) and (26) provide an estimation of the envelope, in the same manner as Eq. (18). Note that using the formula (25) and (26), one can directly demodulate a local AM signal, provided that the factor $|(\sin\Omega_x + \sin\Omega_y)|$ equals one, in other words,

$$\sin\omega_x x_e + \sin\omega_y y_e = \pm 1. \quad (27)$$

According to Eq. (18), the more nearly the factor $|(\sin\Omega_x + \sin\Omega_y)|$ *tends to* 0, the better the error detection will be. Actually this situation implies an indeterminacy (0/0). It corresponds to

$$\omega_x x_e = \omega_y y_e + (2k+1)\pi, \qquad k \in \mathbb{Z}, \quad (28)$$

$$\omega_x x_e = -\omega_y y_e + 2k\pi, \qquad k \in \mathbb{Z}. \quad (29)$$

The previous results show that there exist particular values of (ω_x, ω_y) and (x_e, y_e) for which we expect more efficient demodulations. In Sec. 5 we illustrate such situations in a context of the interferometry.

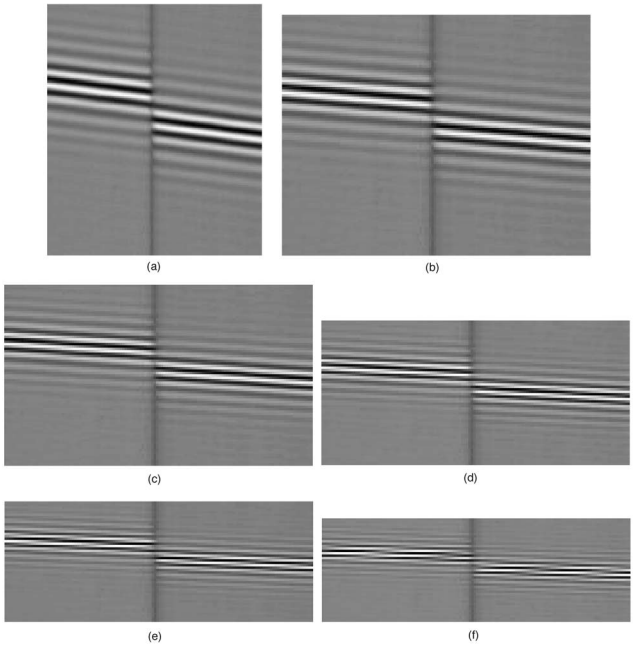

Fig. 2 Real interferometric image at different sampling periods.

4.4.2 *Sampling operator using gradient and Laplacian filters*

In this sub-subsection, we show how the continuous form of the C2DEO allows us to propose a flexible discrete version based on the gradient and Laplacian filters. Let us write Eq. (11) as follows:

$$\Phi_2^c[s(x,y)] = \left(\frac{\partial s}{\partial x} + \frac{\partial s}{\partial y}\right)^2 - s(x,y)\Delta s(x,y) + 2s(x,y)\frac{\partial^2 s}{\partial x\,\partial y}, \tag{30}$$

where Δ is the Laplacian operator. To discretize this equation, we propose to use the well known Prewitt and Sobel filters, which give the derivatives along the vertical and horizontal directions, and the 2-D Laplacian operator.[13] Note that other gradient filters can be used. Let h_x and h_y be the 2-D masks for calculating the derivatives along the x and y axes, respectively. The partial derivatives of an image $(s(i,j))_{1\leqslant i\leqslant N, 1\leqslant j\leqslant N}$ with respect to x and y are given respectively by $s_x(i,j)=h_x * s(i,j)$ and $s_y(i,j)=h_y * s(i,j)$, where $*$ denotes the linear convolution operation. An approximation of $\partial^2 s/\partial x\,\partial y$ is given by the double convolution $s_{xy}(i,j)=h_x * h_y * s(i,j)$. Finally, the discrete version of the C2DEO, denoted D2DEO, is given by

$$\Phi_2^d[s(i,j)] = \{s_x(i,j) + s_y(i,j)\}^2 + 2s(i,j)s_{xy}(i,j) - s(i,j)\{\Delta * s(i,j)\}. \tag{31}$$

Note that instead of differentiating the signal along the rows and columns separately as in Ref. 4, the h_x and h_y filters take into account the local information around each pixel. Maragos and Bovik[4] estimated the discrete amplitude $a(i,j)$ of a local AM-FM signal $s(i,j)=a(i,j)\cos\phi(i,j)$ using

$$|a(i,j)| = \frac{2\Psi_2[s(i,j)]}{\{\Psi_2[s(i+1,j)-s(i-1,j)] + \Psi_2[s(i,j+1)-s(i,j-1)]\}^{1/2}}. \tag{32}$$

Table 1 Sampling period of the interferograms.

Image in Fig. 2	x_e (nm)	y_e (μm)
(a)	40	1.6
(b)	60	1.6
(c)	80	1.6
(d)	100	1.6
(e)	120	1.6
(f)	140	1.6

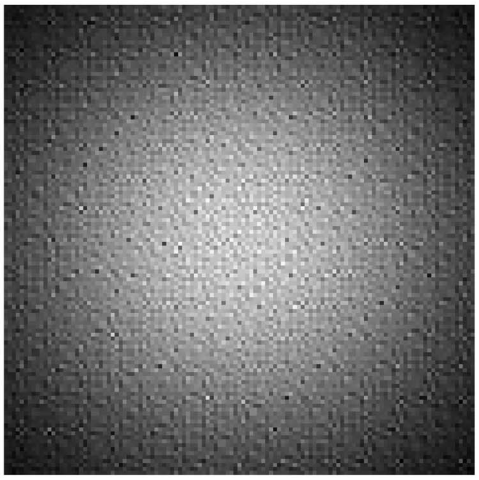

(a)

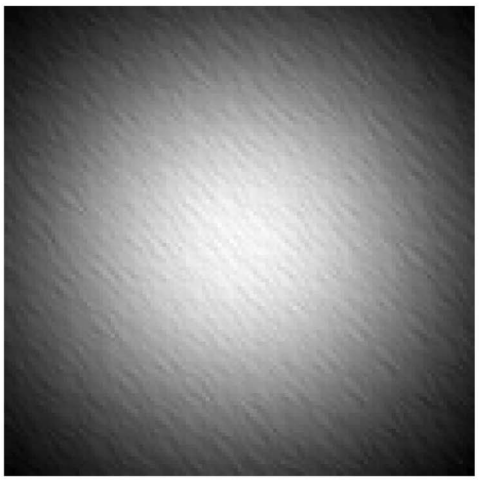

(b)

Fig. 3 (a) Detected envelope with classic 2-D TKEO. (b) Detected envelope with CHOEDA.

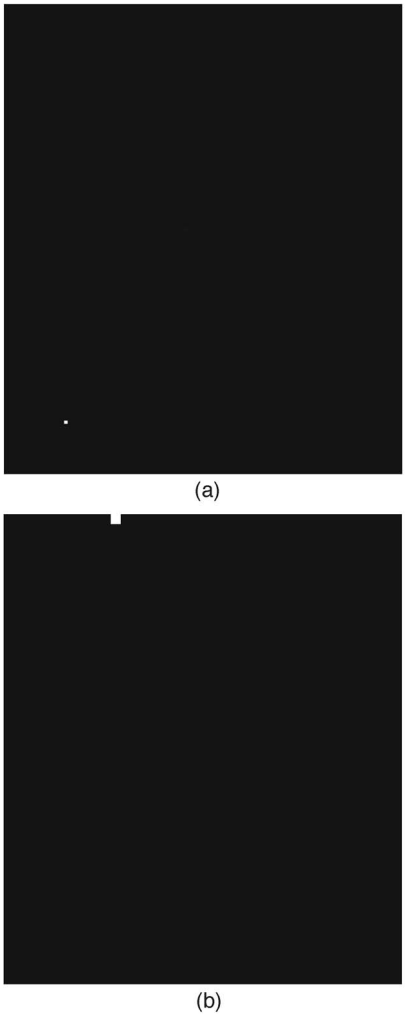

Fig. 4 Detected envelope of the image in Fig. 2(a).

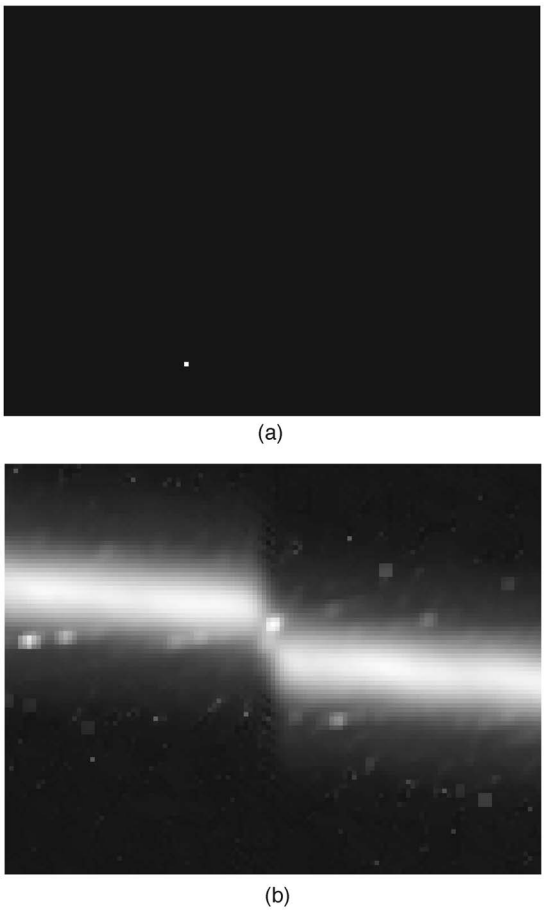

Fig. 5 Detected envelope of the image in Fig. 2(b).

A careful examination of Eqs. (3) and (4) shows that these relations are particular cases of Eq. (31). Under the local AM-signal approximation, we propose in this paper to estimate the local envelope using Eqs. (31), (16), and (18) based on the continuous operators. We again apply gradient filters to compute the different partial derivatives of the signal.

5 Results

5.1 *Simulations*

The CHOEDA is illustrated on synthetic [Fig. 1(a)] and real (Fig. 2) images. We make the assumption that these two images are narrowband signals. Figure 1(a) shows a Gabor wavelet image. This synthetic image corresponds to a carrier sinusoidal signal modulated by a Gaussian envelope shown in Fig. 1(b). The real images, obtained by an interference microscopy system described in Ref. 14, correspond to a series of scanned images of a slanted step of silicon, along the x-depth (row) axis. A single xy image at different sampling periods (see Table 1) was retrieved for use in the present article. This image is a typical 2-D modulated signal of such an optical system. The peak of the fringe envelope along the vertical axis gives the position of the air-layer interface. A general approximation of the intensity along the vertical axis is an AM signal $s(x,y)$ such that $\omega_y \ll \omega_x$. For such images an average wavelength of 640 nm in a white light scanning interferometry system corresponds to a vertical modulation frequency $\nu_x = 1/320\ \mathrm{nm}^{-1}$. Different signal-processing techniques for using coherence probe microscopy (CPM), also known as white light scanning interference microscopy (WLSI), in the measurement of surface roughness have been proposed.[15] Most of the methods are based on an AM signal model, which represents the variation in light intensity measured along the optical axis of an interference microscope. Envelope detection techniques consist of the use of a demodulation procedure[15,16] or measurement of the fringe visibility[17] at a given pixel along the vertical axis x. For example, in Ref. 17, Larkin demodulates such a signal column by column using the well-known five-sample algorithm (FSA), which performs the 1-D discrete Teager-Kaiser operation along the x axis but applied to the differentiated version of the signal. We believe the use of a global approach, such as our method, should be more robust to noise and more competitive in terms of computing time. Our method takes into account the horizontal axis y in order to improve the robustness to noise, and also takes into account the mutual influence between the pixels (due to the

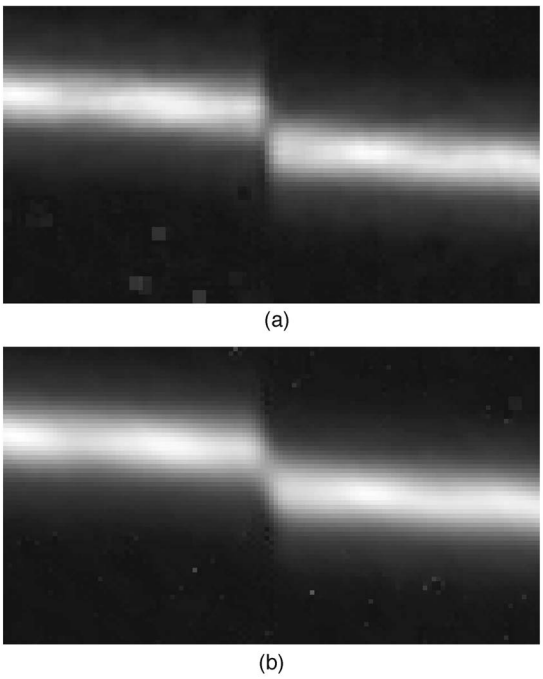

(a)

(b)

Fig. 6 Detected envelope of the image in Fig. 2(c).

point-spread function of the system). Both synthetic and real images are computed, using respectively the classical 2-D TKEO (32), proposed by Maragos and Bovik,[4] and the CHOEDA. The first step of the CHOEDA in estimating the envelope is to compute the second D2DEO (31). The fourth D2DEO is computed using respectively Eqs. (15) and (16). Note that in general it is simpler to estimate the k'th D2DEO using the recurrence (16) than to use direct estimation. Estimated envelopes of synthetic image by CHOEDA method are shown in Fig. 3(b), while the one estimated by the classical 2-D TKEO is shown in Fig. 3(a). One may

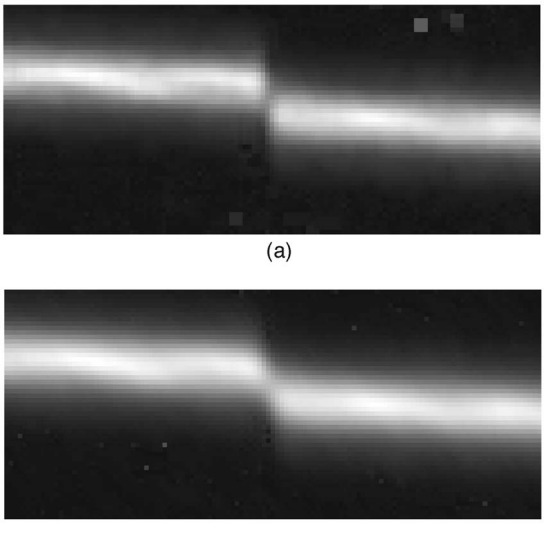

(a)

(b)

Fig. 7 Detected envelope of the image in Fig. 2(d).

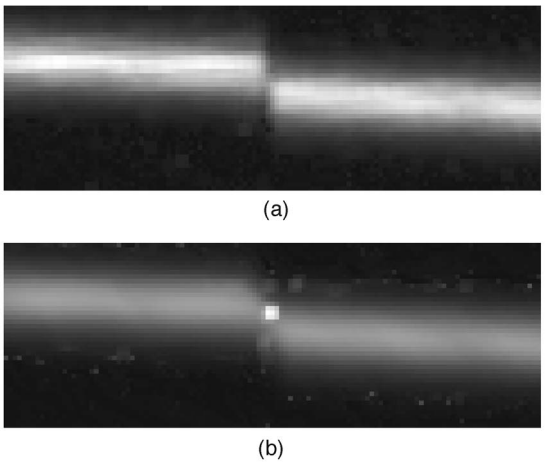

(a)

(b)

Fig. 8 Detected envelope of the image in Fig. 2(e).

note that the envelope of the synthetic image [Fig. 1(b)] is better recovered by the CHOEDA [Fig. 3(b)] than by the classical 2D TKEO [Fig. 3(a)]. This shows the interest in including the diagonal information.

5.2 *Effect of Sampling Frequency*

The sampling step x_e being variable, different extractions of the envelope by the 2DTKEO and the CHOEDA are presented in Figs. 4–9. On one hand, the CHOEDA gives more regular profiles than the approach [Eq. (32)] of Maragos and Bovik[4]: we observe horizontal and vertical directions in the detected envelope using the classical 2-D TKEO [Figs. 6(a), 7(a), and 8(a)], whereas the CHOEDA preserves the diagonal information [Figs. 6(b), 7(b), and 8(b)], so that it gives more homogeneous envelopes. On the other hand, all results confirm an existing link between the sampling step and the quality of the demodulation. At first, for x_e=60 nm, the CHOEDA performs better than the 2DTKEO [see Fig. 5(a) and 5(b)], but this result is reversed for x_e=120 nm [see Fig. 8(a) and 8(b)]. The contrast inversion is due to some points of very high intensity. A careful examination of Fig. 8(b) shows, however, that the envelope is correctly detected. The worst results (Figs. 4 and 9) are for x_e=40 and 140 nm; the best ones (Figs. 5–7) are for x_e

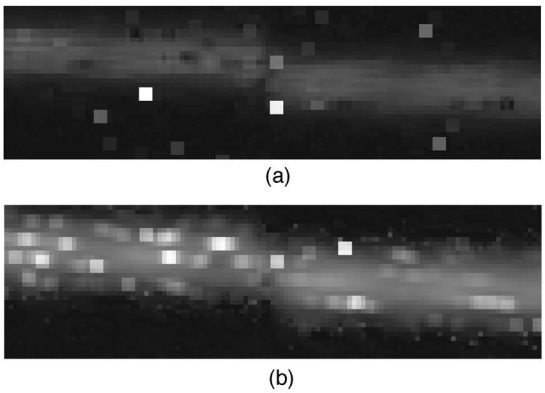

(a)

(b)

Fig. 9 Detected envelope of the image in Fig. 2(f).

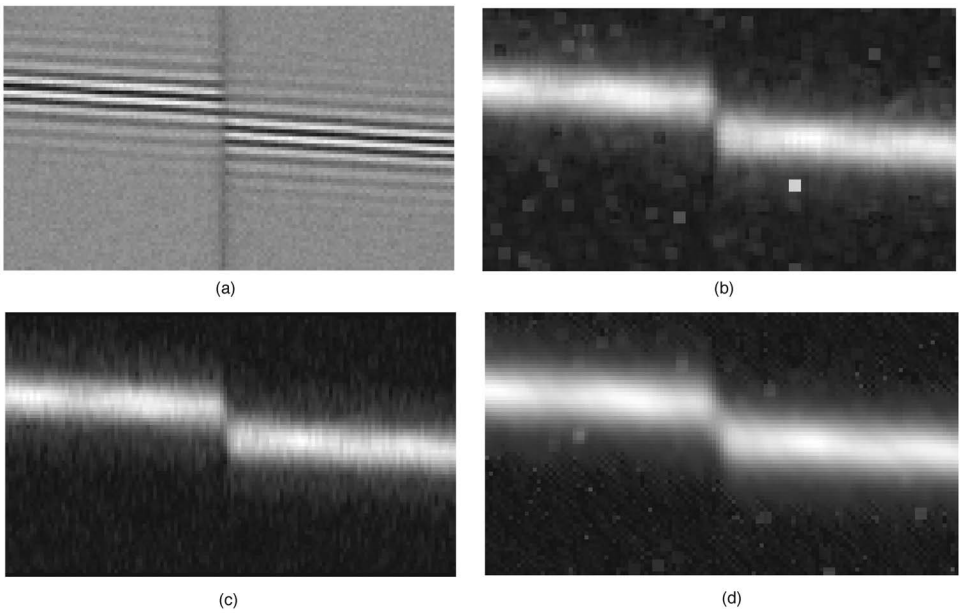

Fig. 10 (a) Noisy version of Fig. 2(c), and detected envelopes using (b) the 2D TKEO, (c) the FSA, and (d) the C2DEO.

=80 and 100 nm. To interpret these results one may refer to Sec. 4.4.1. For such data, a good approximation of the signal $s(i,j)$ is $s(i,j) \approx a(i,j)\cos \Omega_x i = a(i,j)\cos(\omega_x i x_e)$. For a carrier frequency $\nu_x = 1/320$ nm^{-1}, this gives

$$|\sin \omega_x x_e + \sin \omega_y y_e| \approx |\sin \omega_x x_e| = \left| \sin \frac{x_e \pi}{160} \right|. \quad (33)$$

We argue that the discrete model of C2DEO developed in Eqs. (25) and (26) is a good approximation of the discrete model developed in Sec. 4.4.2 using general gradient and Laplacian filters. Thus, good detection depends on the factor given by Eq. (33). The more nearly this factor tends to zero (Fig. 4: x_e=40 nm; Fig. 9: x_e=140 nm), the worse the detection will be. The more nearly this factor tends to one (Fig. 6: x_e=80 nm; Fig. 5: x_e=60 nm; Fig. 7: x_e =100 nm), the better the detection will be.

A complete study of the algorithms, which includes the horizontal sampling, is more complex and not presented in this paper.

5.3 *Robustness to Noise*

Robustness to noise is an important aspect of any AM-FM detection algorithm. The image in Fig. 10(a) represents a noisy version (Gaussian noise) of the image in Fig. 3(c) (with x_e=80 nm). The results shown in Fig. 10(b)–10(d) correspond respectively to the 2-D TKEO, FSA, and CHOEDA algorithms. It is clear that the column-by-column FSA process gives more contrasted envelope than the 2-D demodulation methods. The CHOEDA provides a more homogeneous and less noisy envelope.

6 Conclusions

In this paper, the continuous 2-D Teager-Kaiser and high-order nonlinear operators are introduced. The proposed class of operators takes better into account the diagonal information and is not limited to the sum of the 1-D operators according to the horizontal and vertical directions. Here, we have used image filters to compute the first and second partial derivatives, in order to take into account the spatial context of the pixel. The main application proposed in this work is the image demodulation. More particularly, we focused on envelope detection, which is a typical problem encountered in white light scanning interferometry. The proposed model may also find application in contrast enhancement or image noise filtering. Two continuous higher-order operators, the second and third C2DEOs, are introduced and studied, and a recursive relation between an operator and its predecessors derived. The use of the recursive relation is to generate higher-order operators from lower order ones. The discrete version of the second C2DEO (D2DEO) is proposed and used in the CHOEDA for signal demodulation. The CHOEDA is essentially based on the second and fourth C2DEOs, but other, higher C2DEOs can be used.

The C2DEOs are flexible enough to include many image gradient filters, and thus different discrete versions (D2DEOs) can be obtained. This may be of interest in allowing the choice of a discrete version for a specific application.

As future work we plan to study the C2DEOs for capturing AM-FM information from noisy modulated signals, to perform an analysis of robustness against noise, and also to extend the proposed model for the analysis of multicomponent AM-FM signals.

References

1. P. Maragos, T. F. Quatieri, and J. F. Kaiser, "Energy separation in signal modulations with applications to speech analysis," *IEEE Trans. Signal Process.* **41**, 3024–3051 (1993).
2. J. F. Kaiser, "On a simple algorithm to calculate the energy of a signal," in *Proc. ICASSP*, pp. 381–384, IEEE (1990).
3. T. H. Yu, S. K. Mitra, and J. F. Kaiser, "A novel nonlinear filter for

image enhancement," in *Proc. SPIE/SPSE Symp. on Electronic Imaging: Science and Technology*, pp. 303–309 (1991).
4. P. Maragos and A. C. Bovik, "Image demodulation using multidimensional energy separation," *J. Opt. Soc. Am. A* **12**, 1867–1876 (1995).
5. F. Salzenstein, P. Montgomery, A. Benatmane, and A. O. Boudraa, "2D discrete high order energy operators for surface profiling using white light interferometry," in *Proc. ISSPA*, Vol. 1, pp. 601–604, IEEE, EURASIP (2003).
6. A. C. Bovik, *Image Modulation Models. Handbook for Image and Video Processing*, Academic Press, New York (2000).
7. D. De Vleesschauwer, F. Alaya Cheikh, R. Hamila, and M. Gabbouj, "Watershed segmentation of image enhanced by Teager energy driven diffusion," in *Proc. Sixth Conf. on Image Processing and Its Applications*, pp. 254–258, IEE (1997).
8. S. K. Mitra, H. Li, I. S. Lin, and T. H. Yu, "A new class of nonlinear filters for image enhancement," in *Proc. ICASSP'91*, pp. 2525–2528, IEEE (1991).
9. N. Strobel and S. K. Mitra, "Quadratic filters for image contrast enhancement," in *Twenty-Eighth Asilomar Conf. on Signals, Systems and Computers*, Vol. 1, pp. 208–212, IEEE (1994).
10. G. Ramponi, N. Strobel, S. K. Mitra, and T. H. Yu, "Nonlinear unsharp masking methods for image contrast enhancement," *J. Electron. Imaging* **5**(3), 353–366 (1996).
11. P. Maragos and A. Potamianos, "Higher order differential energy operators," *IEEE Signal Process. Lett.* **2**, 152–154 (1995).
12. E. Kveidalen, "Signal processing using the Teager energy operator and other nonlinear operators," Thesis, Univ. of Oslo (2003).
13. R. C. Gonzalez and R. E. Woods, *Digital Image Processing*, 2nd ed., Prentice-Hall (2002).
14. P. C. Montgomery, A. Benatmane, E. Fogarassy, and J. P. Ponpon, "Large area, high resolution analysis of surface roughness of semiconductors using interference microscopy," *Mater. Sci. Eng., B* **B91-92**, 79–82 (2002).
15. S. S. Chim and G. S. Kino, "Correlation microscope," *Opt. Lett.* **15**, 579–581 (1990).
16. P. J. Caber, "Interferometric profiler for rough surfaces," *Appl. Opt.* **19**, 3438–3441 (1993).
17. K. G. Larkin, "Efficient nonlinear algorithm for envelope detection in white light interferometry," *J. Opt. Soc. Am. A* **13**, 832–843 (1996).

Abdel-Ouahab Boudraa received his BS degree in physics (electronics engineering) from the Constantine Institute of Physics, University of Constantine, Algeria. He received his MS in biomedical engineering from INSA, Lyon, his university degree in nuclear magnetic resonance, his PhD degree in image processing, and his university degrees in statistics and modeling and in positron emission tomography all from the university of Claude Bernard, Lyon 1, France. He is currently an associate professor of electrical engineering at Ecole Navale, Brest, France. His current research interests include computer vision, vector quantization, data structures and analysis, data fusion, time frequency analysis, hard and fuzzy pattern recognition, and applications of fuzzy set theory to medical imaging. He received the 2003 Varian Prize awarded by the Swiss Society of Radiobiology and Medical Physics for the best published paper impacting radiation oncology. He is a member of IEEE.

Fabien Salzenstein received his engineering degree from l'Ecole Nationale Supérieure des Télécommunications de Bretagne, Brest, France. He received his PhD degree in image processing from the University of Rennes 1, in collaboration with Institute National des Telecommunications, Evry, France. He worked as an engineer in Air Traffic Control, Thomson CSF, France. He is currently an associate professor of electrical engineering at the Université Louis Pasteur, Strasbourg, France. His current research interests include data fusion, time frequency analysis, Markovian methods, and fuzzy computer vision applied to astronomy.

Jean-Christophe Cexus received his engineering degree and MSc degree in control from l'Ecole Supérieure des Sciences Appliquées pour l'Ingénieur de Mulhouse (ESSAIM). He is currently pursuing his PhD degree in signal processing at the Institute de Recherche de l'Ecole Navale (IRENav), Brest-Armées, France. His research interests include time-frequency analysis, Sonar target recognition, and neural networks.